In situ high-pressure x-ray diffraction study of icosahedral Al-Cu-TM (TM = V, Cr, Mn) alloys

In situ high-pressure x-ray diffraction study of icosahedral Al–Cu–TM (TM = V, Cr, Mn) alloys

U Ponkratz, R Nicula, A Jianu and E Burkel

Universität Rostock, Fachbereich Physik, August-Bebel-Strasse 55, D-18051 Rostock, Germany

Abstract
Icosahedral Al–Cu–TM (TM: transition metals = V, Cr, Mn) alloys were obtained by single-roller melt-spinning in a protective inert-gas atmosphere. The high-pressure properties up to 20 GPa were investigated by *in situ* energy-dispersive x-ray diffraction at a synchrotron source using a gas-membrane diamond-anvil cell. No phase transitions could be observed. The bulk modulus of the Al–Cu–TM quasicrystalline phases was found to increase with the Hume-Rothery factor. Moreover, the bulk modulus of the quasicrystalline phase is imposed by the bulk modulus of the transition metal element. The derived values for the first pressure derivative B_0' indicate strong anharmonic contributions in the lattice potentials.

1. Introduction

Although the high-temperature stability of icosahedral alloys has been studied quite extensively, only a few investigations have so far been concerned with the high-pressure behaviour of these alloys. The first high-pressure experiments were performed on the meta-stable binary alloy Al–Mn which was shown to be stable under pressures as large as 28 GPa [1]. The bulk modulus and its first pressure derivative were found to be $B_0 = 117.6$ GPa and $B_0' = 6$. The first high-pressure investigations on icosahedral Al–Cu–TM and Al–Pd–TM (TM: transition metal) alloys were performed in the middle of the 1990s. Energy-dispersive x-ray diffraction experiments on Al–Cu–Fe ($B_0 = 165$ GPa and $B_0' = 1.15$) [2], Al–Cu–Ru ($B_0 = 128$ GPa and $B_0' = 5$) [3], Al–Pd–Mn ($B_0 = 133$ GPa and $B_0' = 5$) [4] and Al–Pd–Re ($B_0 = 180$ GPa and $B_0' = 5$) [3] samples demonstrated the stability of these alloys up to pressures as high as 35 GPa. In a more recent study, Al–Pd–Mn was shown to be stable up to 70 GPa [5]. All studies were performed on stable icosahedral phases. In contrast, ternary metastable alloy systems of the Al–Cu–3d-TM group have not been the subject of detailed high-pressure investigations so far. A question arises of whether a metastable icosahedral alloy can be transformed to a stable crystalline or to an amorphous phase under high pressure. Our study was further motivated by the question of how strong the influence of the transition metal on the compression behaviour of icosahedral alloys is: the formation of icosahedral phases is influenced by the density of conduction electrons per atom e/a, also known as the Hume-Rothery factor [6]. In Al–Cu–3d-TM alloys, the Hume-Rothery factor increases with

increasing atomic number Z of the transition metal [6]. The atomic number Z increases in the order V $\rightarrow$ Cr $\rightarrow$ Mn $\rightarrow$ Fe $\rightarrow$ Co. Al–Cu–V, Al–Cu–Cr and Al–Cu–Mn form metastable icosahedral phases only and Al–Cu–Fe ($e/a = 1.8$) is the only stable quasicrystal from the Al–Cu–3d-TM group. This is the stability limit for the formation of icosahedral phases: Al–Cu–Co forms a decagonal alloy.

2. Experimental procedures

The alloys with compositions $Al_{62}Cu_{25.5}TM_{12.5}$ were prepared by the single-roller melt-spinning method in a protective Ar atmosphere. The resulting as-quenched alloys were ribbons 1 to 10 cm long with an average cross-section of 2 mm $\times$ 50 μm. Fine grains of the as-quenched material were obtained by dry grinding in an agate mortar and were employed in the high-pressure experiments. The *in situ* high-pressure SR diffraction experiments were performed at the F3 beamline of the DESY/HASYLAB Synchrotron Radiation Laboratory (Hamburg, Germany) using the white beam delivered by a bending-magnet radiation source ($E_c = 16.6$ keV). The scattered radiation was recorded by a Ge solid-state detector (Princeton Gamma-Tech). We used a rather small scattering angle, $\Theta \approx 3.7°$. The energy of the Ge detector ranges from 13 to 68 keV; with the scattering angle mentioned above, momentum transfers up to 4.5 Å^{-1} could be reached. Before each run the diffraction angle was determined using a gold foil. Additional details on the set-up of the F3 HASYLAB beamline can be found elsewhere [7]. Pressures were generated by a gas-membrane diamond-anvil cell (DIACELL DXR-GMW), equipped with 500 μm diameter diamonds. The sample powders were loaded together with a methanol/ethanol (4:1) mixture as the pressure-transmitting medium. Samples were enclosed in a 200 μm diameter hole drilled in a 200 μm thick Inconel gasket, preindented to about 50 μm. Pressures were determined using the ruby fluorescence scale [8]. Cahn (N, M) indices [9] were used for indexing the i-phase diffraction lines. The indexing procedure allows for the evaluation of the hypercubic lattice constant, a_6, according to

$$q = \frac{1}{d_{N,M}} = \frac{1}{a_6} \frac{\sqrt{N + M\tau}}{\sqrt{2(2 + \tau)}} \tag{1}$$

where q is the parallel space momentum transfer, τ is the golden mean, $d_{N,M}$ is the interplanar distance for the (N, M) i-phase diffraction line and a_6 is the hypercubic lattice parameter. The positions of the diffraction lines were determined by profile fitting with Pearson-VII functions. To calculate the hypercubic lattice parameter, for each spectrum the values of $\sqrt{(N + M)}$ were plotted versus energy. The slope is indirectly proportional to the hypercubic lattice parameter a_6 which is determined using a linear least-squares fit. The pressure dependence of the sample volume was followed by monitoring the relative change of the d-spacings of the i-phases. Pressure-dependent volume ratios can consequently be calculated from the i-phase d-spacings according to $V/V_0 = [a_6(p)/a_6(p_0)]^3$ (isotropic compression assumption). The zero-pressure bulk modulus, B_0, and its pressure derivative, B_0', were determined from a least-squares fit to a second-order Birch equation of state (EOS) [10]:

$$p = \frac{3}{2} B_0 \left[\left(\frac{V}{V_0} \right)^{-7/3} - \left(\frac{V}{V_0} \right)^{-5/3} \right] \left[1 + \frac{3}{4}(B_0' - 4) \left[\left(\frac{V}{V_0} \right)^{-2/3} - 1 \right] \right]. \tag{2}$$

3. Results

Indexing of the zero-pressure i-phase diffraction patterns leads to following hypercubic lattice constants : $a_6 = 6.56 \pm 0.02$ Å for Al–Cu–V, $a_6 = 6.494 \pm 0.008$ Å for Al–Cu–Cr and

$a_6 = 6.396 \pm 0.003$ Å for Al–Cu–Mn. The agreement with the values reported by Popescu *et al* [6] are in each case better than 0.5%. The widths of the diffraction lines were found to be rather broad (FWHM: $\approx$0.5 keV to 0.7 keV) compared to the resolution function of the experimental set-up (FWHM: $\approx$0.35 keV for 25 keV photons). Since the relative energy resolution $\delta E/E$ of an energy-dispersive spectrometer is best at diffraction angles in the region of $\Theta \approx 2°$ [11], a rather small diffraction angle of $\Theta \approx 3.7°$ was chosen. With this diffraction angle, reflections up to (20, 32) are accessible. The x-ray diffraction patterns of all three samples show clearly the reflections (6, 9), (7, 11), (11, 16), (18, 29) and (20, 32) which could be followed up to the highest pressures applied. For the Al–Cu–Cr and Al–Cu–Mn samples the (8, 12) reflection could also be observed for all pressures. Since there are no signs of a phase transition to a crystalline or an amorphous high-pressure phase, the metastable Al–Cu–TM alloys can be regarded as stable under pressure. Diffraction patterns of the three samples are shown in figure 1. Besides the reflections from the quasicrystalline phase, all spectra showed reflections that could not be indexed according to an icosahedral symmetry. These reflections are most probably due to admixture of crystalline phases and marked with c in figure 1. Furthermore, the diffraction patterns show reflections from the Inconel gasket (marked with g) and tungsten fluorescence lines (marked with W) arising from the beam collimation system.

The fit results for the Al–Cu–V sample gave $B_0 = 79$ GPa ± 6 GPa and $B_0' = 10.7 \pm 1.6$. The measurements on Al–Cu–Cr show a bump in the p–V relation in the pressure range from 7 to 14 GPa. This is probably due to due to the solidification of the pressure-transmitting medium and/or to a bridging effect of the sample material between the diamond anvils. Consequently, data points in this pressure range were excluded when fitting the equation of state. For the equation of state we found $B_0 = 122$ GPa ± 2 GPa and $B_0' = 12 \pm 1$. Al–Cu–Mn could be compressed up to 14 GPa. We found for the bulk modulus $B_0 = 116$ GPa ± 7 GPa, and for the first pressure derivative $B_0' = 9.5 \pm 2$. The relative volumes V/V_0 for the three alloys, together with the corresponding Birch fits, are shown in figure 2. The hypercubic lattice parameters, the atomic radii of the transition metal from reference [12], the Hume-Rothery factors from [6], the bulk moduli and their pressure derivatives for the Al–Cu–TM alloys are compiled in table 1; for comparison reasons the bulk modulus and the first pressure derivative for Al–Cu–Fe from reference [2] were also added.

Table 1. Hypercubic lattice parameter a_6, atomic radius of the transition metal r_{TM}, Hume-Rothery factor e/a, bulk modulus B_0 and first pressure derivative B_0' for Al–Cu–TM alloys.

Sample	Al–Cu–**V**	Al–Cu–**Cr**	Al–Cu–**Mn**	Al–Cu–**Fe**
a_6 (Å) (reference [6])	—	6.480(1)	6.415(1)	6.335(1)
a_6 (Å) (present work)	6.56(2)	6.494(8)	6.396(2)	—
r_{TM} (Å) (reference [12])	1.338	1.276	1.268	1.260
e/a	$\approx$1.5	1.56	1.68	1.80
B_0 (GPa)	79 ± 6	122 ± 2	116 ± 7	165 ± 10
B_0'	10.7 ± 1.6	12 ± 1	9.5 ± 2	1.15 ± 0.6

4. Discussion

The metastable icosahedral Al–Cu–3d-TM phases are more compressible than the stable phases from the Al–Cu–TM group. Al–Cu–Fe has a bulk modulus of $B_0 = 165$ GPa; the bulk modulus of the stable alloy containing the 4d transition element ruthenium, Al–Cu–Ru, was found to be $B_0 = 128$ GPa. The bulk modulus of the metastable Al–Cu–3d-TM alloys increases with
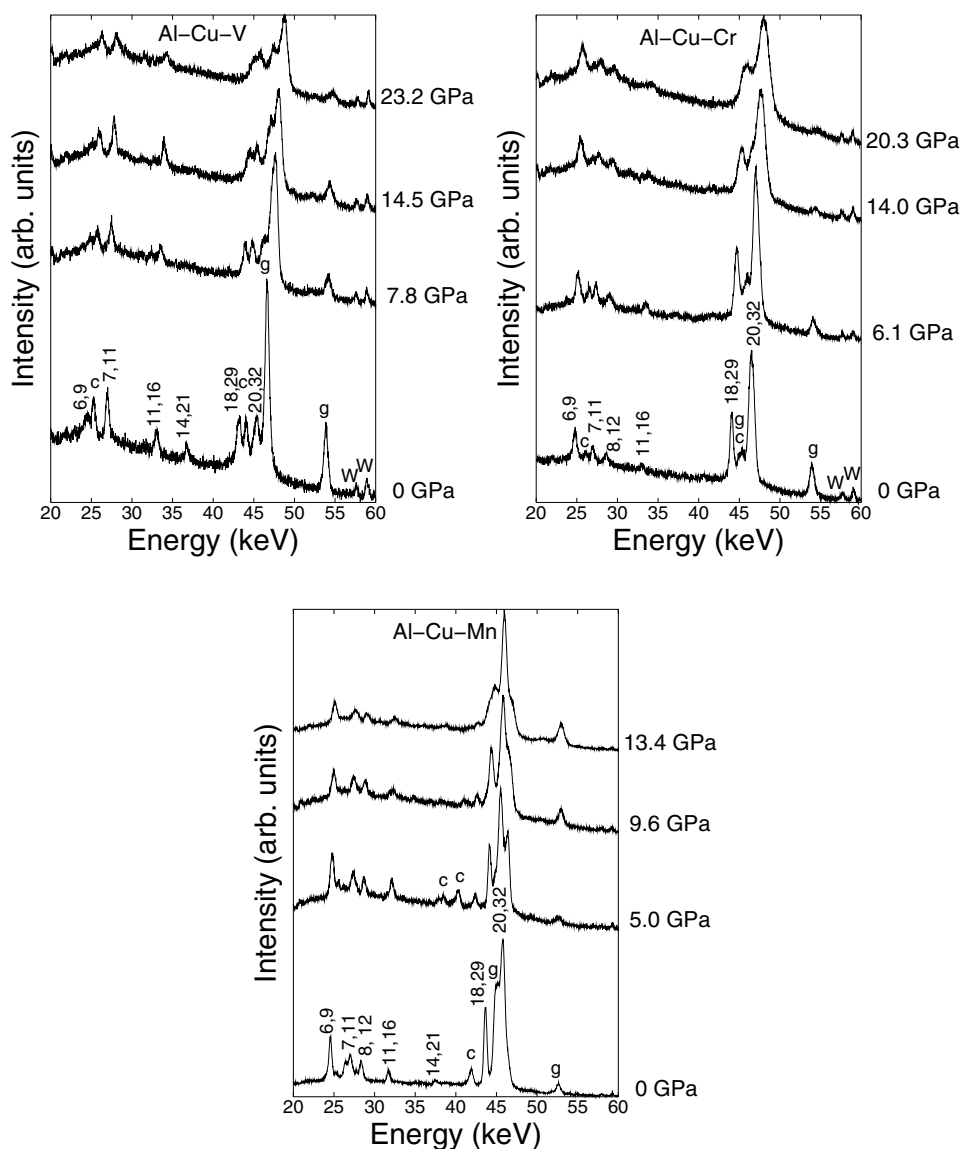
Figure 1. Energy-dispersive x-ray diffraction patterns of Al–Cu–V, Al–Cu–Mn and Al–Cu–Cr at various pressures.

increasing atomic number of the transition metal. We can correlate the increasing bulk modulus in the V $\rightarrow$ Cr $\rightarrow$ Mn $\rightarrow$ Fe series with the increasing Hume-Rothery factor. One would consequently expect Al–Cu–Mn to have a bulk modulus higher than that of Al–Cu–Cr and lower than that of Al–Cu–Fe. However, Al–Cu–Mn is an exception, having a bulk modulus of 116 GPa which is slightly lower than that of Al–Cu–Cr. Here it is useful to compare the bulk moduli of the pure transition elements [13]: V, Cr and Fe show almost the same bulk modulus of about 160 GPa, again Mn being an exception with a bulk modulus of 90.4 GPa; see table 2.

Larger bulk moduli might also be related to an enhanced packing density of the Al–Cu–TM alloy series. Comparing the data from table 1 one finds that both the hypercubic lattice
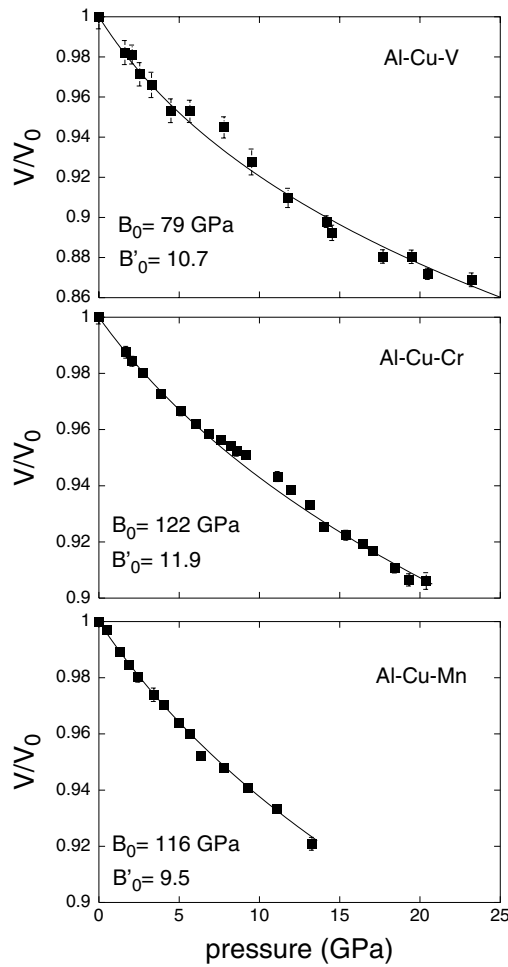
Figure 2. Compression curves for the Al–Cu–TM alloys with corresponding fits to a Birch equation of state.

Table 2. Bulk moduli of the transition elements V, Cr, Mn and Fe [13].

Transition element	V	Cr	Mn	Fe
Atomic number	23	24	25	26
B_0 (GPa)	155	160	90.4	163

parameter a_6 and the atomic radius r_{TM} of the transition element decrease with increasing atomic number, in almost identical manners, so the packing density is a slowly varying function of the atomic number of the transition metal and almost does not influence the bulk modulus of the quasicrystals. Moreover, it was previously shown [14] that the relative structural stability of the $Al_{12}TM$ icosahedral cluster, the basic building block of the archetypal quasicrystalline structure, is strongly dominated by electronic effects while the size of the TM element contributes only to a much lesser extent.

Comparing the bulk moduli of Al–Pd–Mn ($B_0 = 133$ GPa) and Al–Pd–Re ($B_0 = 180$ GPa) with the bulk moduli of the transition metals Mn ($B_0 = 90.4$ GPa) and Re ($B_0 = 360$ GPa)

[13], Hasegawa *et al* [5] suggested that the compression properties of icosahedral alloys may be related to those of the constituent transition metal. Our results show that the bulk modulus of the metastable icosahedral alloys is indeed strongly influenced by the bulk modulus of the transition element. Our measurements additionally indicate that the electronic configuration of the whole system, reflected by the Hume-Rothery factor e/a, plays a main role.

One can also try to compare the compression properties of Al–Cu–Fe with those of the stable icosahedral phase Al–Cu–Ru. Since Fe has the same number of d electrons as Ru, the resulting alloys Al–Cu–Fe and Al–Cu–Ru have the same Hume-Rothery factor. However, the compression properties of Al–Cu–Ru do not fit into the above proposed scheme: exchanging the element Fe ($B_0 = 163$ GPa) with Ru ($B_0 = 303$ GPa) [13] should lead to a higher bulk modulus for Al–Cu–Ru compared to Al–Cu–Fe. This is not the case: Al–Cu–Ru was shown to be more compressible ($B_0 = 128$ GPa) than Al–Cu–Fe ($B_0 = 165$ GPa) [2, 3].

Furthermore, Al–Cu–V, Al–Cu–Cr and Al–Cu–Mn show large values for their first pressure derivatives (values close to 10). In contrast, Al–Cu–Fe has a low value of B_0' of only 1.15. In ordinary metals, the value for the first pressure derivative B_0' is close to 4. Large values for the first pressure derivative may be attributed to anharmonic terms of the quasilattice lattice potential. These high values may be related to the fact that we are dealing with metastable systems, i.e. systems not in thermodynamical equilibrium.

A high value $B_0' = 11 \pm 3$ was also found in high-pressure experiments on nanocrystalline CdS [16]. Nano-CdS undergoes a phase transition from a fourfold- to a sixfold-coordinated structure at approximately 6 GPa, whereas bulk CdS already shows this transition at a pressure of about 6 GPa. Between 3 GPa and 6 GPa, the wurtzite structure is not the thermodynamically stable phase; in the pressure range above 3 GPa the NaCl structure has a lower Gibbs free energy. However, in the case of nano-Cds, the fourfold structure is stabilized by surface energy contribution terms which cannot be neglected for nanostructured materials. The p–V relation for nanocrystalline PbS also suggests unusually large B_0'-values; unfortunately the exact fit results are not given in the original reference [16]. In metastable or nanostructured materials, high pressures may be used to probe the anharmonic terms of the lattice potential which are reflected by an increased hardening under pressure; i.e. by a large value for B_0'.

5. Conclusions

High-pressure experiments yielded that Al–Cu–TM icosahedral phase (TM = V, Cr, Mn) alloys are stable up to applied pressures close to 20 GPa. The compression properties of quasicrystalline alloys are not only determined by the compressibility of the constituent transition metals, but also by the electronic configuration of the whole system: the bulk moduli of the icosahedral phases were found to increase with increasing Hume-Rothery factor. The values for the first pressure derivatives B_0' are quite large. This may be related to strong anharmonic terms of the lattice potential in metastable alloys.

References

[1] Sato-Sorensen Y and Sorensen L B 1989 *Phys. Rev.* B **39** 2654
[2] Lefebvre S, Bessiere M, Calvayrac Y, Itié J P, Polian A and Sadoc A 1995 *Phil. Mag.* B **72** 101
[3] Sadoc A, Itié J P, Polian A, Berger C and Poon S J 1998 *Phil. Mag.* A **77** 115
[4] Amazit Y, Perrin B, Fischer M, Itié J P and Polian A 1997 *Phil. Mag.* A **75** 1677
[5] Hasegawa M, Tsai A P, Kondo T, Yagi T and Kikegawa T 1999 *J. Non-Cryst. Solids* **250–252** 849
[6] Popescu R, Jianu A, Manciu M, Nicula R and Manaila R 1995 *J. Alloys Compounds* **221** 240
[7] Otto J W 1997 *Nucl. Instrum. Methods* A **143** 551
[8] Mao H K, Bell P M, Shaner J W and Steinberg D J 1978 *J. Appl. Phys.* **49** 3276
[9] Cahn J W, Shechtman D and Gratias D 1986 *J. Mater. Res.* **1** 13
[10] Birch F 1978 *J. Geophys. Res.* **83** 1257
[11] Buras B and Gerward L 1989 *Prog. Cryst. Growth Charact.* **18** 93
[12] Pauling L 1960 *The Nature of the Chemical Bond* (Ithaca, NY: Cornell University Press) p 403
[13] Young D A 1991 *Phase Diagrams of the Elements* (Berkeley, CA: University of California Press)
[14] Carlsson A E 1991 *Phys. Rev.* B **43** 12 176
[15] Tolbert S H and Alivisatos A P 1994 *Nanophase Materials* ed G C Hadjipanayis and R W Siegel (Dordrecht: Kluwer Academic) p 471
[16] Qadri S B, Yang J, Ratna B R, Skelton E F and Hu J Z 1996 *Appl. Phys. Lett.* **69** 2205